Phase Stability and Fast Ion Conductivity in the Hexagonal LiBH4-LiBr-LiCl Solid Solution

Phase Stability and Fast Ion Conductivity in the Hexagonal $LiBH_4$-LiBr-LiCl Solid Solution

Valerio Gulino,[a)b)] Matteo Brighi,[b)] Erika M. Dematteis,[a)] Fabrizio Murgia,[b)] Carlo Nervi,[a)] Radovan Černý,[b)] and Marcello Baricco[a)*]

[a)] Department of Chemistry and Inter-departmental Center Nanostructured Interfaces and Surfaces (NIS), University of Turin, Via Pietro Giuria 7, 10125 Torino, Italy

[b)] Laboratoire de Cristallographie, DQMP, Université de Genève, quai Ernest-Ansermet 24, CH-1211 Geneva 4, Switzerland

*Corresponding author

Marcello Baricco

E-mail address: marcello.baricco@unito.it

Tel.: +39 011 6707569

Fax: +39 0116707856

Supporting Information Description

Figure S1: Table and plot of prepared samples.

Figure S2: PXD pattern as a function of temperature of sample s4.

Figure S3: Rietveld refinement of sample s1.

Figure S4: HP-DSC signal of sample s3.

Figure S5: PXD pattern of sample s2 to verify long-time stability

Figure S6: PXD pattern as a function of milling time of sample s3.

Figure S7: Density as a function of composition.

Figure S8: Activation energy as a function of volume.

Samples preparation

In the table and in **Figure S1** the samples prepared and the conditions of the synthesis are reported.

Sample Name	Composition (Molar Fraction)			Synthesis & Treatments
	$LiBH_4$	LiBr	LiCl	
s1	0.33	0.33	0.33	BM 1.5 h + AN 2h 250 °C
s2	0.38	0.33	0.29	BM 1.5 h + AN 2h 250 °C
s3	0.38	0.33	0.29	BM 1, 2, 4, 6, 22, 24, 41 h
s4		0.50	0.50	BM 1.5 h
s5	0.80	0.20		BM 1.5 h + AN 4h 250 °C
s6	0.70	0.30		BM 1.5 h + AN 2h 250 °C
s7	0.60	0.40		BM 1.5 h + AN 2h 250 °C
s8	0.50	0.50		BM 1.5 h + AN 2h 250 °C
s9	0.40	0.60		BM 1.5 h + AN 2h 250 °C
s10	0.60	0.20	0.20	BM 1.5 h + AN 2h 250 °C
s11	0.22	0.58	0.20	BM 1.5 h + AN 2h 250 °C
s12	0.22	0.19	0.59	BM 1.5 h + AN 2h 250 °C
s13	0.60	0.10	0.30	BM 1.5 h + AN 2h 250 °C
s14	0.21	0.69	0.10	BM 1.5 h + AN 2h 250 °C
s15	0.40	0.40	0.20	BM 1.5 h + AN 2h 250 °C
s16	0.40	0.50	0.10	BM 1.5 h + AN 2h 250 °C
s17	0.49	0.41	0.10	BM 1.5 h + AN 2h 250 °C
s18	0.50	0.30	0.20	BM 1.5 h + AN 2h 250 °C
s19	0.50	0.20	0.30	BM 1.5 h + AN 2h 250 °C
s20	0.60	0.30	0.10	BM 1.5 h + AN 2h 250 °C
s21	0.70	0.20	0.10	BM 1.5 h + AN 2h 250 °C

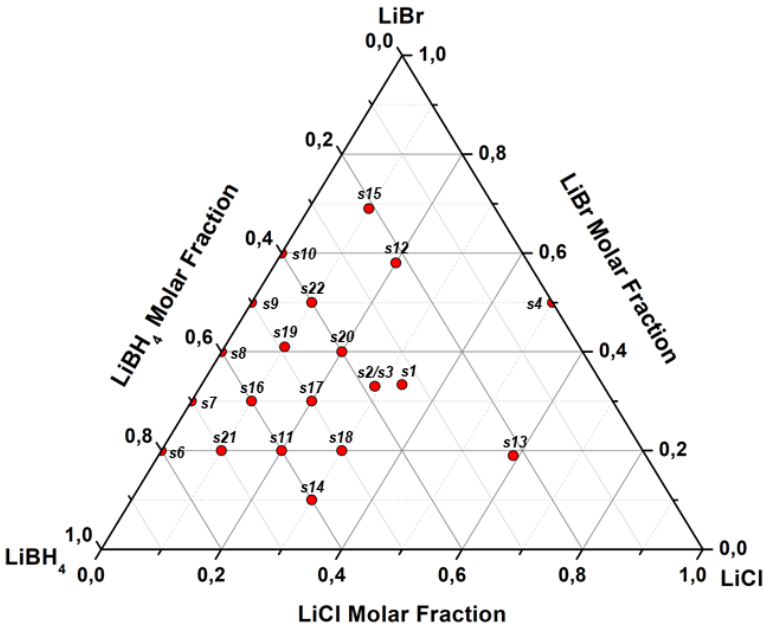

Figure S1. *Composition plot for all samples prepared. Preparation methods and compositions of the investigated samples are indicated in the table. Ball milled (BM) time is reported, together with annealing (AN) time and temperature.*

Verification of the Vegard's law for the LiBr-LiCl cubic solid solution

The LiBr-LiCl phase diagram reported in literature,[1] presents a complete solid solution with no miscibility gap and a liquidus curve with a thermal minimum at 522 °C, y_{LiCl} = 0.36.
An equimolar mixture of LiBr and LiCl (sample ***s4***) was prepared to verify the Vegard's law in the LiBr-LiCl binary system. An i*n situ* high-temperature X-ray Powder Diffraction (XPD) measurement was performed on $(LiBr)_{0.5}(LiCl)_{0.5}$ (Bragg-Brentano geometry) into Aanton-Paar XRK 900 reactive chamber, under dynamic vacuum. Patterns were collected in a temperature range *RT* < T < 400 °C with a heating/cooling rate of 5 °C/min. In order to remove the presence of water in the powder, a preliminary annealing at 120 °C for 10 h was performed. Calcium Oxide (CaO, purity >99% from Sigma-Aldrich) was used as internal standard.
Analysing by X-ray diffraction the $(LiBr)_{0.5}(LiCl)_{0.5}$ (sample ***s4***) as function of temperature (**Figure S2**), the cell parameter of $Li(Br)_{1-x}(Cl)_x$ solid solution has been determined. A cubic solid solution is formed at 250 °C, resulting stable down to *RT*, confirming the calculated phase diagram.[1] The cell parameter obtained by Rietveld refinement does follow the Vegard's law.

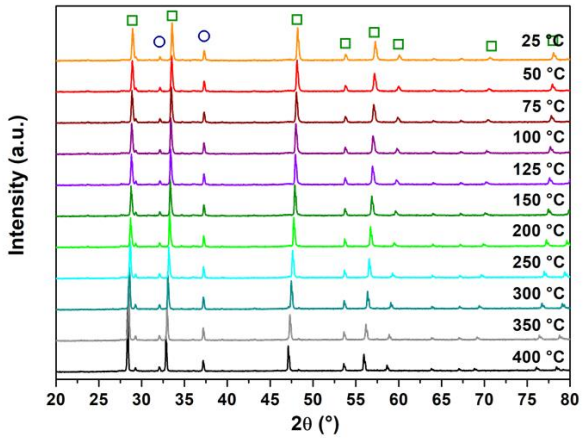

Figure S2. *X-ray diffraction pattern as a function of temperature for sample s4. Symbols: blue circles CaO and green squares* $Li(Br)_{1-x}(Cl)_x$.

Rietveld refinement of sample s1 after AN

Using the solution of equation (2) it was possible to refine the pattern. The sample after AN contains 14 wt.% of solid solution $LiBr_{0.28}Cl_{0.72}$ and 86 wt.% of h-$Li(BH_4)_{0.39}Br_{0.33}Cl_{0.2}$.

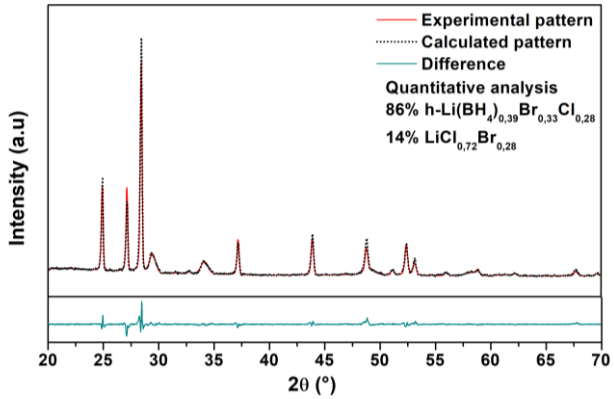

Figure S3. *Results of the Rietveld refinement of XPD pattern of sample* ***s1*** *after AN. (Rwp 11.66 %,* χ *2.10).*

HP-DSC signal of sample s2

The HP-DSC signal confirms that all $LiBH_4$ is in the hexagonal phase as solid solution, considering that the transition peak of $LiBH_4$ is not present.

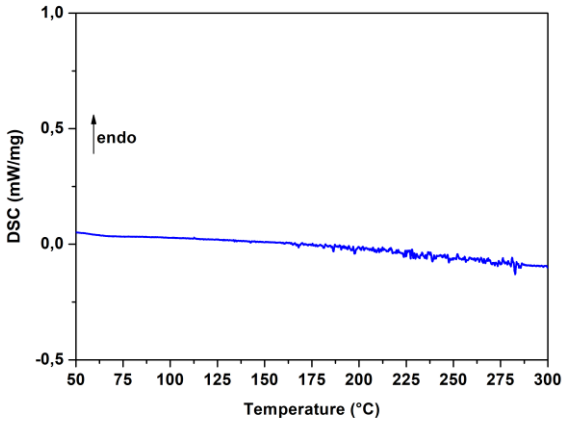

Figure S4. *HP-DSC signal of sample* ***s2*** *after ball milling. The ramp used was form 30 °C to 300 °C at 5°C/min under 10 bar of* H_2*.*

Stability of the solid solution evaluated over time

The stability of the solid solution of sample s2 was evaluated over time, i.e. after about one-year. The pattern obtained after one year corresponds to that of the as-prepared sample.

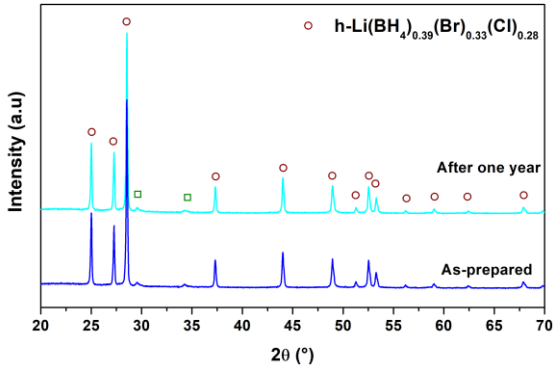

Figure S5. *X-ray diffraction pattern of sample s2 after AN preparation (bottom) and after one year (top). Symbols indicate the cubic and hexagonal solid solutions.*

Effect of the milling time on the formation of the solid solution.

Different patterns were collected for different time of milling for the sample s3, with the same composition as the sample s2. t0 indicates the pattern of the hand-mixed sample.

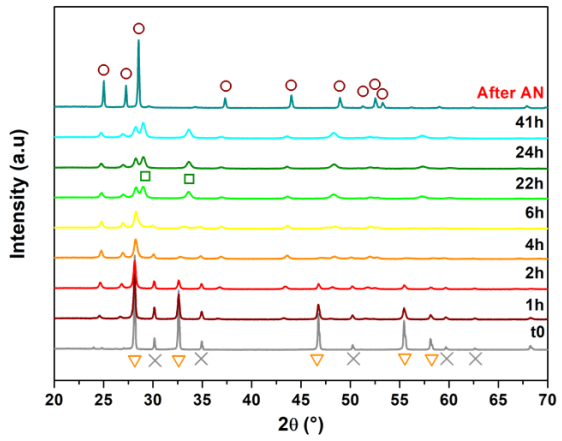

Figure S6. *Effect of the milling time on sample s3. Symbols: triangles LiBr, cross LiCl, circles h-Li(*BH_4*)$_{1-\alpha-\beta}$(Br)$_\alpha$(Cl)$_\beta$, squares Li(Br)$_{1-\varepsilon}$(Cl)$_\varepsilon$.*

Density map as a function of composition

The density (ρ) of the samples was evaluated using the occupancy of the *2b* site of h-$LiBH_4$, the weight of the anion and the obtained cell volume. Figure S7b shows conductivity at *RT* as a function of $1/\rho$. The samples highlighted have the best proprieties for possible technological applications.

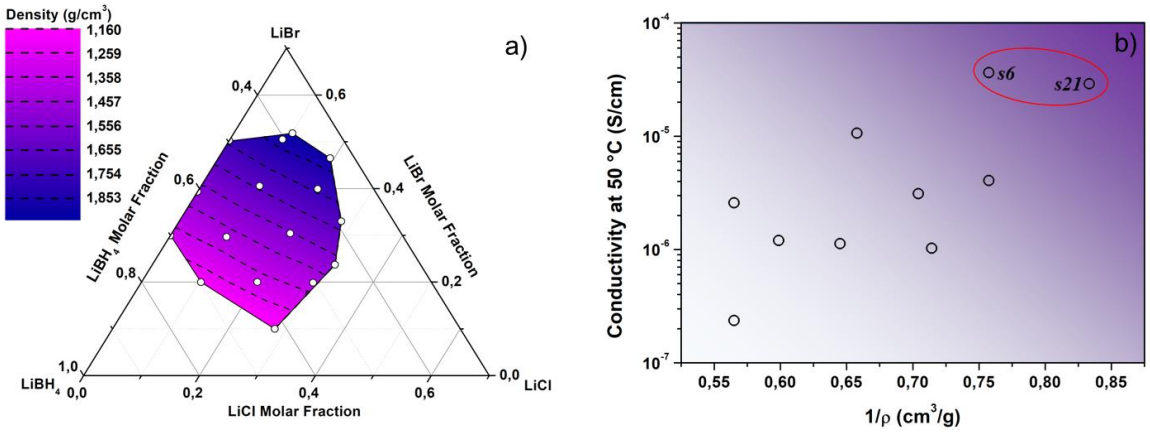

Figure S7. *(a) Contour map of density of samples in the hexagonal solid solution in the* $LiBH_4$*-LiBr-LiCl system as a function of composition. Iso-density dashed lines correspond of the values and lines shown in the legend. (b) plot of Li-ion conductivity at 50 °C with respect to the inverse of the density. The oval highlights the samples having a low density and, at the same time, a high conductivity.*

Activation energy as a function of volume

Figure S8 shows the activation energy as a function of the obtained volume for h-Li$(BH4)_{1-\alpha-\beta}(Br)_{\alpha}(Cl)_{\beta}$ monophasic samples. The activation energy increases with volume decreases, indicating that also the dimension of the lattice is influence on the transport proprieties of the system.

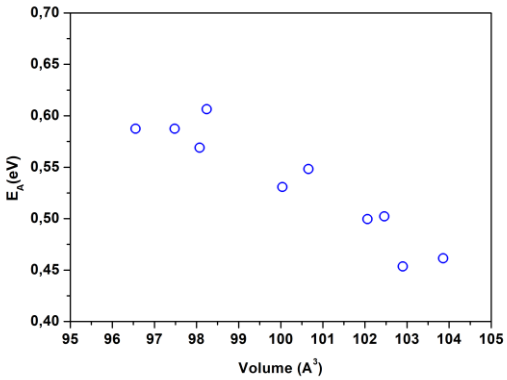

Figure S8. *Activation energy of h-Li$(BH4)_{1-\alpha-\beta}(Br)_{\alpha}(Cl)_{\beta}$ monophasic samples, as a function of the unit cell volume.*

References

(1) J. Sangster, A. P. Phase Diagrams and Thermodynamic Properties of the 70 Binary Alkali Halide Systems Having Common Ions. *J. Phys. Chem. C* **1987**, *16*, 511–561.